LIGHT SCATTERING AND PARTICLE AGGREGATION IN SNOW-STORMS

By Malcolm Mellor

(U.S. Army Cold Regions Research and Engineering Laboratory, Hanover, New Hampshire, U.S.A.)

Abstract. Attenuation of visible radiation by falling snow was studied by a method based on brightness contrast between topographic features and the adjacent sky. Extinction coefficient and visual range are related to bulk snow density, and are compared with data for Antarctic blizzards. Since attenuation depends more on the size and concentration of discrete particles than on the mass density of suspended snow, the process of particle aggregation and snow-flake formation during fall is considered by collision theory, and an expression describing aggregation effects is developed. This offers an explanation for the relative constancy of particle concentration observed at ground level during snowfalls of varying intensity. Since there is no strong justification for relating extinction coefficient to snow density, an empirical correlation between extinction coefficient and precipitation rate is given for practical use. It is shown that visual range estimated by eye in hilly terrain may be less than the true value, since sky brightness is locally reduced over broad hill-tops with low albedo.

Résumé. *Dispersion de la lumière et aggrégation de particules dans les tempêtes de neige.* L'atténuation par la neige en chute de la radiation visible est étudiée selon une méthode basée sur le contraste de luminosité entre les traits topographiques et le ciel au-dessus. Le coéfficient d'extinction et la portée visuelle sont mise en relation avec la densité de la neige, pour être comparés avec les données des blizzards antarctiques.
Puisque l'atténuation dépend de la dimension et de la concentration des particules discrètes plutôt que de la densité-masse de la neige en suspension, le procédé de l'aggrégation est envisagé en termes de la théorie de la collision, dont l'Auteur développe une expression descriptive des effets de l'aggrégation.
Cette expression offre une explication de la constance relative de la concentration des particules observée au niveau du sol pendant des chutes de neige d'intensités différentes.
Dans l'absence d'argument probant en faveur d'une relation entre le coefficient d'extinction et la densité de la neige, l'Auteur offre une corrélation empirique entre le coefficient d'extinction et le taux de précipitation, convenable à l'usage courant.
Il est démontré que l'oeil humain, en estimant sa portée visuelle sur des terrains accidentés, tend à sous-estimer les valeurs à cause de la réduction locale de la luminosité au-dessus des sommets larges ayant un albédo faible.

Zusammenfassung. *Lichtstreuung und Teilchenballung in Schneestürmen.* Die Verringerung der sichtbaren Strahlung bei Schneefall wurde anhand der Helligkeitsunterschiede zwischen topographischen Gegenständen und dem benachbarten Himmel untersucht. Der Extinktionskoeffizient und die Sichtweite werden in Beziehung zur Schneedichte gebracht und mit den Daten antarktischer Schneestürme verglichen. Da die Verringerung mehr von der Grösse und Konzentration diskreter Teilchen abhängt als von der Massendichte fallenden Schnees, wird die Teilchenballung und Schneeflockenbildung während des Fallens vom Standpunkt der Kollisionstheorie betrachtet und es wird ein Ausdruck zur Beschreibung des Ballungseffektes entwickelt. Damit ergibt sich eine Möglichkeit, die verhältnismässig konstante Teilchenkonzentration zu erklären, die man am Boden bei unterschiedlich starkem Schneefall beobachtet hat. Da es keinen überzeugenden Grund gibt, den Extinktionskoeffizienten auf die Schneedichte zu beziehen, wird für den praktischen Gebrauch eine empirische Wechselbeziehung zwischen diesem und der Niederschlagsmenge angegeben. Es wird gezeigt, dass die mit dem Auge geschätzte Sichtweite in hügeligem Gelände kleiner sein kann, als ihr wahrer Wert, da die Helligkeit des Himmels über breiten Hügelrücken mit niedriger Albedo örtlich vermindert ist.

Introduction

When practical questions concerning attenuation of visible radiation by falling snow were raised, cursory search of the literature revealed little relevant information. In view of the complex shape of snow particles a purely theoretical approach seemed undesirable, and so an immediate attempt was made to measure the attenuation of light transmitted through falling snow from a diffuse source. This proved unsatisfactory, since the photometric device available at that time was insufficiently sensitive for work over the necessarily short ($\sim$100 m.) transmission path. Interim working estimates of extinction coefficient were therefore made from visibility data for Antarctic blizzards, supplied prior to publication by Radok (see Budd and others, in press).

During the remainder of the winter (1964–65) simple measurements of visual range were made for a variety of conditions experienced at Hanover, N.H., and some control measurements were made with a telephotometer. These data have provided information on light

237

attenuation by falling snow, and have also given rise to some interesting speculations regarding particle aggregation during snowfall.

It appears that useful studies in this area of interest can be made with very simple equipment, so that the type of work described here may commend itself to field glaciologists as a foul-weather occupation.

LIGHT SCATTERING AND BRIGHTNESS CONTRAST

As an alternative to measuring beam attenuation directly, extinction coefficients for falling snow may be determined by considering the reduction of brightness contrast between a dark target and the adjacent horizon sky. Relevant theory, originated by Koschmieder and reviewed by Middleton (1952), Johnson (1954) and others, is outlined below.

Consider a cone of vision directed horizontally through a uniform field of snow-filled air. The cone is illuminated uniformly, say by sunlight diffused through a dense overcast. Snow particles in a representative elementary volume of the cone scatter light (independently and incoherently), so that the element has a brightness, or luminance, B_h which is determined by the incident illumination and by the number and nature of the snow particles. B_h is the intrinsic brightness of the snow-filled element, but the apparent brightness sensed by an observer at the apex of the cone of vision is reduced by scattering in the intervening snow cloud. In the cone, luminous flux and brightness do not change with distance from the apex x if the air is perfectly clear; brightness B diminishes with x only because of scattering from snow particles, and attenuation follows the Bouger–Lambert law:

$$\frac{dB}{B} = -\sigma \, dx \tag{1}$$

where σ is the extinction coefficient, or, since absorption is probably negligible for snow, the scattering coefficient. It is assumed independent of x. In general σ is a function of wave-length, but since snow particles are very large compared with the wave-length of visible radiation it is expected to be almost independent of wave-length in the visible range. Solution of equation (1) with the condition $B = B_h$ when $x = 0$ yields:

$$B = B_h \exp(-\sigma x). \tag{2}$$

When the line of sight is directed through an effectively infinite thickness of the snow cloud, i.e. towards the horizon sky, the total apparent brightness sensed by the observer B_{ah} is found by integrating throughout the cone between the limits $x = 0$ and $x = \infty$:

$$B_{ah} = B_h \sigma \int_0^\infty \exp(-\sigma x) \, dx = B_h. \tag{3}$$

When the line of sight is directed instead to a "black" target of zero luminance, horizontal distance X from the observer, the total apparent brightness sensed by the observer B_{at} is:

$$B_{at} = B_h \sigma \int_0^X \exp[-\sigma x] \, dx = B_h[1 - \exp(-\sigma X)]. \tag{4}$$

If the target is not black, but has an intrinsic brightness B_0, the apparent brightness sensed by the observer B_{at}' is the brightness of the limited cone B_{at} plus the attenuated brightness of the target itself:

$$B_{at}' = B_h[1 - \exp(-\sigma X)] + B_0 \exp(-\sigma X). \tag{5}$$

The apparent contrast C between a distant target of sufficient size and the horizon sky is:

$$C = \frac{B_{at}' - B_h}{B_h}. \tag{6}$$

The intrinsic contrast C_0 between the target and the adjacent horizon sky as $X \to 0$ is:

$$C_0 = \frac{B_0 - B_h}{B_h}. \tag{7}$$

C_0 may take values from -1 for a black body up to positive values for self-luminous targets. Equation (5) can now be re-written in terms of brightness contrast:

$$C = C_0 \exp(-\sigma X), \tag{8}$$

or

$$\sigma = \frac{1}{X} \ln\left(\frac{C_0}{C}\right). \tag{9}$$

If we define a visual range V as the distance X between observer and target at which apparent contrast C diminishes to the minimum level distinguishable by eye (termed the liminal contrast ϵ), then equation (9) becomes a relation between extinction coefficient and visual range. It has been found that under a wide range of daylight conditions the average human eye can discern a target of adequate size (say greater than 1° visual angle) if the apparent contrast exceeds 2 per cent. From this there follows a standard definition of the meteorological visual range V_m as the maximum distance at which the average eye can distinguish a black target of suitable size, i.e. with $C_0 = -1$ and $\epsilon = -0.02$,

$$V_m = \frac{3.912}{\sigma}. \tag{10}$$

MEASUREMENTS OF VISIBILITY AND BRIGHTNESS CONTRAST

Simultaneous measurements of visual range and bulk snow density (mass of snow per unit atmospheric volume) were made on all occasions when conditions were judged to be suitable according to the following criteria: (i) sky completely overcast, (ii) little or no wind, (iii) snow density steady with time and distance for the duration of an observation (snow squalls were not sampled). Visual range was estimated by using as targets a succession of pine-covered hills and ridges, all of similar height to the observation point. The vertical mass flux of snow was measured by exposing a tray for a timed interval and weighing the catch. The mean vertical component of snow particle velocity was measured by timing the fall of particles through a height of approximately 3 m. at several different locations. With some care and practice this measurement could be made consistently simply by following particles, or groups of particles, by eye and timing their fall with a stop-watch. Snow density was obtained by dividing the vertical mass flux by the fall velocity.

In the latter part of the study period attempts were made to measure number density as well as mass density. When falls were predominantly of simple single particles the number flux could be obtained by exposing a tray for a brief timed period (about 10 sec.) and then counting the particles seen through 10 windows of a template laid over the tray. Snow-flakes and other fragile aggregations of particles usually shattered into their components on hitting the tray, but late in the study it was found that the required flux estimates could be made by exposing a warmed tray for about 5 sec. and counting the water marks. The simultaneous measurements of mass flux and number flux for single particle falls yielded estimates of mean particle mass for various types of snow crystals.

Photometric control readings were made with a Spectra brightness meter, model UB $1\frac{1}{2}$, with stabilized power source and external galvanometer. The meter accepts light from a 1.5° solid angle. Target brightness was compared with the brightness of adjacent horizon sky for several targets lying at distances of 15 m. to 3.1 km. Readings were made using a filter which simulates the spectral response of the human eye, and also with blue ($\approx 0.445\ \mu$) and red ($\approx 0.585\ \mu$) filters. The extinction coefficient was obtained graphically in accordance with equation (9). Results of observations are tabulated in the Appendix.

ATTENUATION AS A FUNCTION OF DENSITY

This work was originally intended to determine extinction coefficient for falling snow and to relate it to some descriptive index such as snow density or precipitation rate. Before proceeding to this end result, however, it seems desirable to enquire into the justification for such relationships.

Results from standard electromagnetic theory provide a relation which expresses the scattering coefficient for spherical aerosols as the total effective scattering area per unit volume:

$$\sigma = KNa \tag{11}$$

where N is the number of particles per unit volume, a is the cross-sectional area of a particle normal to the beam, and K is the scattering area ratio, i.e. the area of wave front affected by a particle divided by the actual particle area a (strictly speaking, particle size distribution should be taken into account by writing the summation $\sigma = \sum_{i=1}^{n} K_i N_i a_i$, but here we seek simplicity).

The numerical concentration of particles N in falling or blowing snow is not easy to measure, but the mass density γ can be obtained without too much trouble. It is therefore convenient to express N as a function of γ, at least for simple particle shapes:

$$N = \frac{A_1 \gamma}{l^3 \gamma_i} \tag{12}$$

where l is a characteristic linear dimension of the particle, γ_i is ice particle density, and A_1 is a dimensionless constant. The particle cross-section a is proportional to l^2, so that equation (11) can be re-written as:

$$\sigma = \frac{A_2 K_l \gamma}{l \gamma_i} \tag{13}$$

where the geometric coefficient A_2 is constant for a given shape of particle and the scattering parameter K_l is a function of particle size and shape, though perhaps a weak function in view of the large particle size for snow.

As a preliminary to examination of the data for gently falling snow, we may quickly review existing data on visual range during blizzard conditions.

When cold snow is blown by strong winds the grains are usually equant and often rounded; the particle size and the size distribution at a height of 2 m. or so apparently vary rather little from time to time and place to place. Under these circumstances A_2, K_l and l are constants, and a linear relation between σ and γ is to be expected. Visibility data for Antarctic blizzards by Budd and others (in press) show that this is indeed the case (Fig. 1), and therefore it is entirely logical to express σ as a function of γ for blowing snow. Since Budd and others give particle sizes it is possible to calculate the approximate value of K_l. If it is assumed that the visibility estimates were in accordance with the meteorological standard,* i.e. $C_0 = -1$ and $\epsilon = 0 \cdot 02$, values of K_l between $1 \cdot 8$ and $2 \cdot 7$ are obtained, depending on how l is defined for the non-spherical particles.† These values may be compared with the limiting value of 2 given by Mie theory (Middleton, 1952; Johnson, 1954).

When snow is falling in relatively calm weather, the size and shape of crystals and flakes vary widely with atmospheric conditions, and it would be surprising if σ remained simply related to γ. However, while $A_2 K_l/l$ is not likely to be constant, there could still be linear correlation between σ and γ if $A_2 K_l/l$ does not vary systematically with γ. The data of Figure 1

---

* This assumption is not strictly justifiable, since the stakes used for targets were neither black nor sufficiently wide. However, Liljequist's (1957) data for blizzard visibility as a function of wind speed indirectly support the measurements of Budd and others.

† It may be taken as one half of either the "effective diameter" or the "projective diameter" of equivalent spheres; with a spherical approximation in which l is a radius, $A_2 = \frac{3}{4}$.
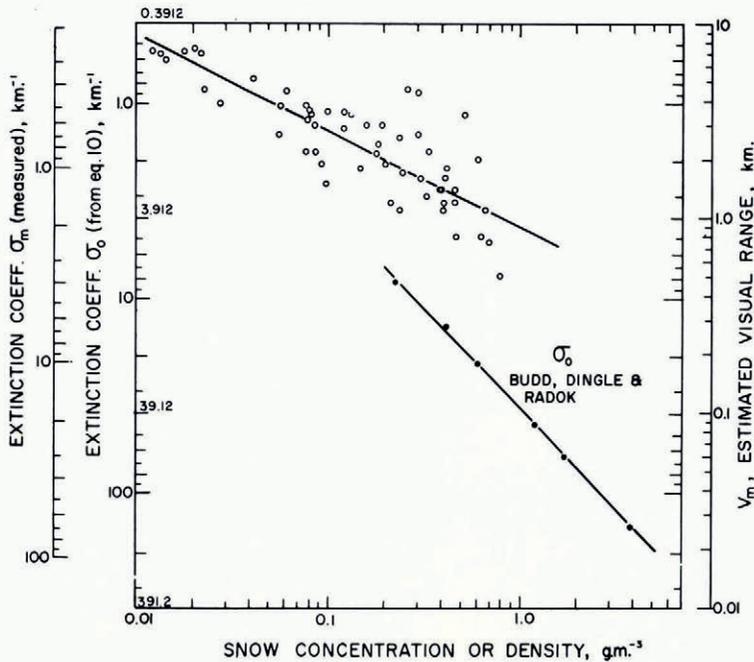
Fig. 1. Extinction coefficient and visual range related to the density of suspended snow. Note that a direct comparison of σ_0 for the Antarctic blizzard with σ_m for falling snow brings the data into coincidence for the mid-range of densities

dispel this possibility; any relation between σ and γ is clearly non-linear. A first guess from the logarithmic plot is that σ might be proportional to γ^n, where $n \leqslant \frac{2}{3}$.

The difficulty at this point is that there is no prima facie evidence for a simple relation between γ and the total scattering area Na. It becomes necessary to consider how particle size and concentration vary for snow-storms generally.

CONCENTRATION AND AGGREGATION OF FALLING SNOW PARTICLES

As a starting point for this discussion, we explore the implications of the power relation between σ and γ mentioned above. The most clearly defined limit of the data in Figure 1 gives a maximum value of the exponent $n \approx \frac{2}{3}$, and if equation (13) is appropriately rearranged we see that this value implies that $\gamma^{\frac{1}{3}}$, and hence from equation (12) $N^{\frac{1}{3}}$, is constant, or at least does not vary appreciably with γ. In Figure 2, $N^{\frac{1}{3}}$ is plotted against γ, and it can be seen that overall there is no significant correlation. With the exception of one set of observations the values of $N^{\frac{1}{3}}$ vary rather little over the observed range of conditions. Since $N^{\frac{1}{3}}$ is a relatively weak function there is greater variation in the values of N, but nevertheless it seems legitimate to consider whether N is kept within certain limits by some mechanism.

First of all, it may be recalled that nucleation of ice crystals from supercooled cloud droplets usually requires freezing nuclei, which are typically kaolinite particles from terrestrial dust. In some geographical locations the concentration of freezing nuclei may be fairly constant over the winter period, although the efficiency of nucleation apparently depends to some extent on temperature. If N were held between fairly narrow limits by availability of freezing nuclei, then the density of falling snow would be determined by the mass of the individual particles. Crystal form and size depend on temperature and degree of super-saturation of the atmosphere, and in general there is a correlation between air temperature
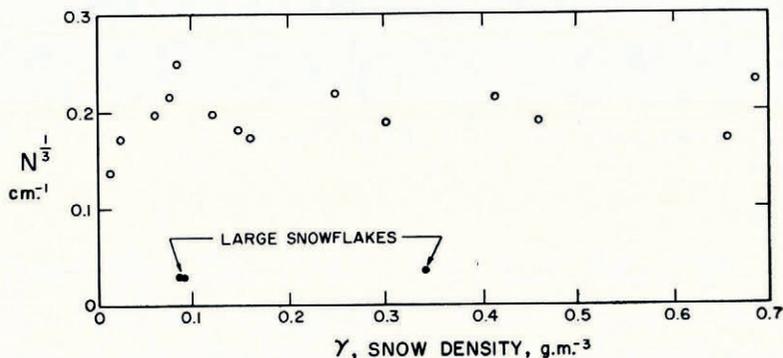
Fig. 2. $N^{\frac{1}{3}}$ plotted against snow density

at an observation station and the size of snow crystals encountered there. Intensity of snowfall also tends to be related to air temperature, but it is not known whether there is a correlation between particle size and intensity of snowfall. Using the very rough data from the present observations, and checking estimated crystal masses against Mason's (1962) data for generally larger crystals, particle mass has been plotted against snow density in Figure 3. There is little apparent correlation, although a systematic trend might still be found with more precise data and wider sampling. Group averages of the data suggest a slight increase of particle mass as density increases.

So far no mention has been made of particle aggregation, although light scattering depends on the concentration of discrete particles rather than the absolute number of crystals present. Winters at Hanover are cold, and heavy snowfall with large flakes is quite rare, but on one occasion when large snow-flakes fell with temperatures near the freezing point the concentration of flakes was relatively low—about two orders of magnitude smaller than typical concentrations for snowfall in the cold weather. Visual range on this occasion was abnormally
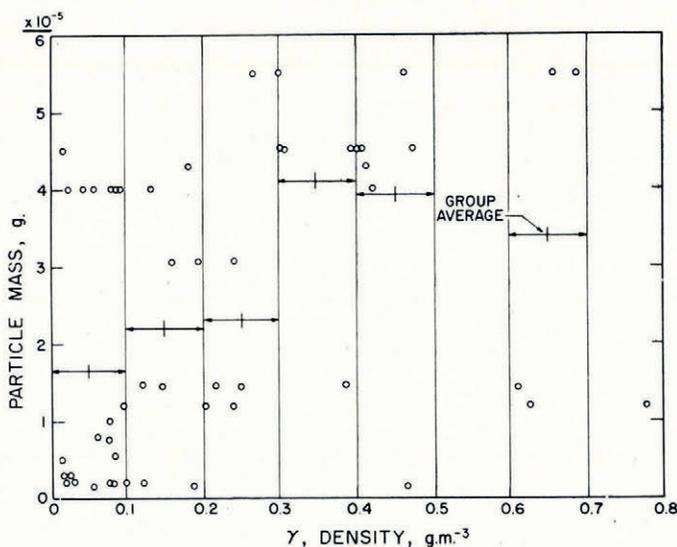
Fig. 3. Mean mass of single snow particles plotted against snow density

great for snow of that density. We should therefore give some thought to the collision process by which flakes and other aggregations are formed.

Consider a large unit volume which encloses many falling particles and which moves downward at the mean fall velocity of the enclosed particles. In general, neighbouring particles move relative to each other; size, shape, and hence fall velocity, of individual particles vary, and aerodynamic instability of planar crystals causes "fluttering" oscillations. Free-air turbulence is probably unimportant, as it tends to produce in-phase displacement over relatively large volumes. A mean free path for the particles $\bar{L}$ may be defined as:

$$\bar{L} = \frac{1}{N\bar{a}_c} \tag{14}$$

where $\bar{a}_c$ is a mean "collision cross-section" for the particles. This will probably correspond closely to the geometric cross-section, although it could be defined to accommodate the effects of any net electrostatic attractions.

We introduce a "wandering velocity" $\bar{v}$, which is the deviation from the mean fall velocity of all the particles, determined largely by the shape and size distribution of the particles. The frequency of collision for a particle f is therefore:

$$f = \frac{\bar{v}}{\bar{L}}. \tag{15}$$

When two particles collide they may simply rebound, or they may adhere to form a single larger particle. The probability of adhesion will be determined by the geometry of the colliding grains and by the physical state of their surfaces; intricate dendrites will readily interlock, and warm crystals with high specific surface or extreme local curvature will adhere tenaciously. To express the proportion of collisions which result in adhesion we introduce an "aggregation efficiency" E.

It is now possible to write an expression for the rate at which particles are removed in effect from the cloud by collision and adhesion:

$$\frac{dN}{dt} = -EN\frac{\bar{v}}{\bar{L}}. \tag{16}$$

$\bar{L}$ is actually a function of N, but we now assume that the collision cross-section of two adhering particles is the sum of their individual cross-sections and so, since $N\bar{a}_c$ is constant, $\bar{L}$ becomes constant for a given snowfall.

If particles fall from their parent cloud with initial concentration N_0 at time $t = 0$, the solution of equation (16) is:

$$\left. \begin{aligned} N &= N_0 \exp\left(-\frac{E\bar{v}t}{\bar{L}}\right), \\ N &= N_0 \exp\left(-EN_0\,\bar{a}_{c0}\,\bar{v}t\right). \end{aligned} \right\} \tag{17}$$

or

Hence the concentration of discrete particles N diminishes exponentially with time during fall and the rate constant for the decay depends on the size of individual particles, on the "wandering velocity", and on the aggregation efficiency.

An interesting aspect of equation (17) is the way in which N at ground level varies with initial concentration N_0 when other parameters are held constant; no matter how abundant the particles at the cloud base, in general the concentration at ground level is limited. This is illustrated in Figure 4 for a range of values of $(E\bar{a}_{c0}\,\bar{v}t)$ chosen to conform with the following estimates of magnitudes: $E \sim 10^{-1}$ to 1, $\bar{a}_{c0} \sim 10^{-4}$ to 10^{-1} cm.^{2}, $\bar{v} \sim 10$ cm./sec., $t \sim 10^3$ sec. On these assumptions there is virtually no aggregation of very small particles during a typical fall, but large stellar dendrites aggregate so fast that the concentration of resulting snow-flakes at ground level can never be very high.

The mid-winter snowfalls observed in Hanover typically had spatial dendrites of about 0·5 mm. diameter, and assuming these to have an aggregation efficiency of about 0·8 the corresponding value of $(E\bar{a}_{c_0} \bar{v}t)$ is 20. For this condition interpolation on Figure 4 shows only a slow change of N with N_0; the actual curve (not plotted in Fig. 4) traverses the range of observed values for N (5×10^{-3} to 15×10^{-3} cm.$^{-3}$). Since mass density γ is a measure of N_0 for a given type of snow, we thus have a possible explanation for the apparent constancy of N with γ which prompted this discussion.

For the rare falls of large (5 mm.) stellar dendrites mentioned above, the value of $(E\bar{a}_{c_0} \bar{v}t)$ is about 10^3 cm.$^{-3}$. Although the curve for this value is unplottable on the scale of Figure 4, it gives the maximum concentration N after a fall of 10^3 sec. of order 10^{-4} cm.$^{-3}$, which may be compared with the observed snow-flake concentrations of 2 to 4×10^{-5} cm.$^{-3}$.
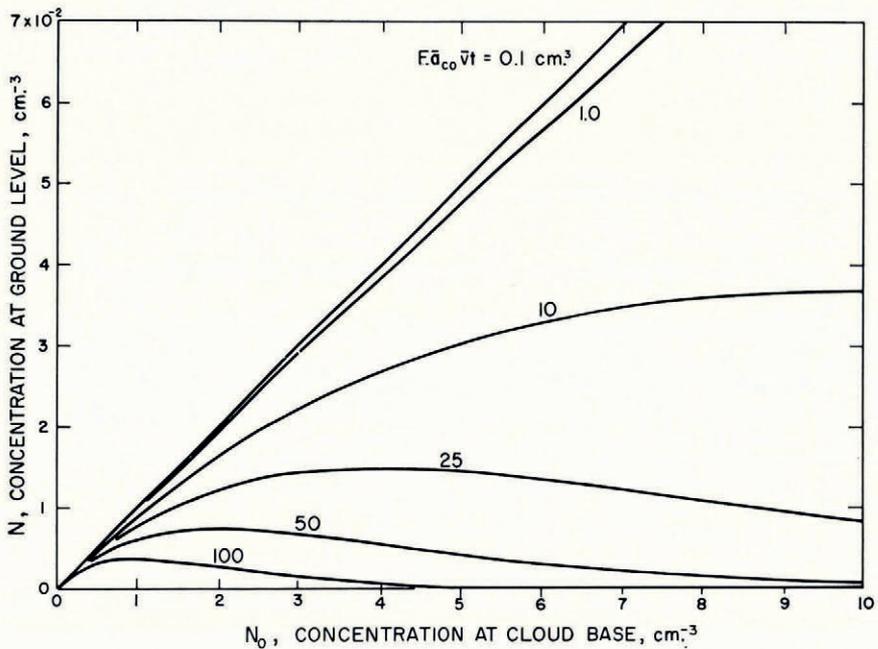
Fig. 4. *Concentration of discrete particles at ground level (N) as a function of particle concentration at the base of the parent cloud (N_0), according to equation (17)*

PRESENTATION OF LIGHT ATTENUATION DATA

In view of the foregoing it seems unprofitable to fit an empirical regression line to the data of Figure 1. In fact, for practical purposes there seems to be no special merit in relating extinction coefficient to snow density if a wide range of snow types has to be accommodated. Since fall velocity does not vary greatly (Fig. 5), it is just as satisfactory, and much more convenient, to relate extinction coefficient to the more easily measureable precipitation rate. This procedure is, of course, only applicable when snow is falling directly in calm weather.

Figure 6 shows the correlation between visual range and snow accumulation rate and also between extinction coefficient and snow accumulation rate. The regression line yields the relations:

$$V_m = 0·625 A^{-0·421} \tag{18}$$

where V_m is in km. and A, the snow accumulation rate, is in g. cm.$^{-2}$ hr.$^{-1}$;

$$\sigma_0 = 6·26 A^{0·421} \tag{19}$$
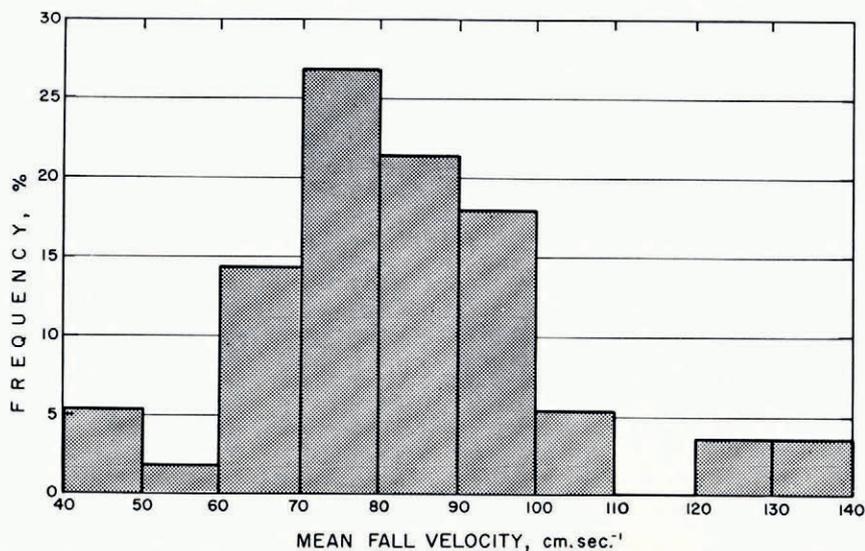
Fig. 5. Histogram giving frequency distribution for snow particle and snow-flake fall velocity (covering all observations made at Hanover, N.H., during winter of 1964/65)
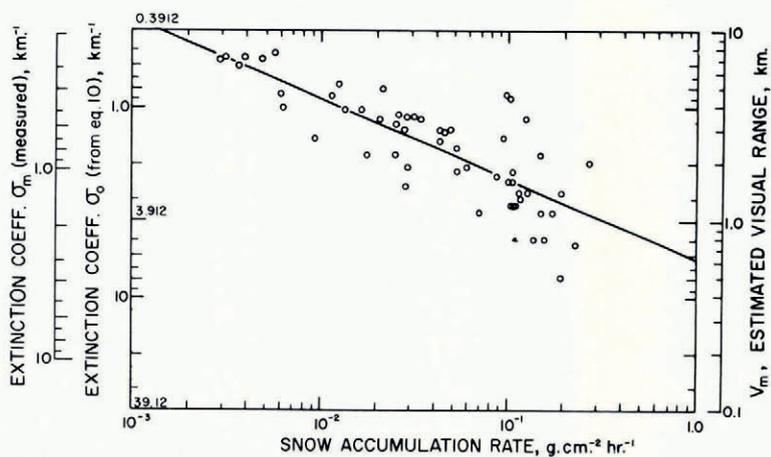
Fig. 6. Extinction coefficient and visual range related to snow accumulation rate for snow falling in wind-free conditions

where σ_0, the extinction coefficient according to equation (10), is in km.$^{-1}$ and A is in g. cm.$^{-2}$ hr.$^{-1}$. The extinction measurements made photometrically show that σ_0 is actually about twice the true value for extinction coefficient; for the range of conditions checked by control measurements the true extinction coefficient σ_m follows the relation:

$$\sigma_m = 0.467\sigma_0 = 2.92A^{0.421} \text{ km.}^{-1}. \tag{20}$$

The exponent in (19) and (20) is approximately equal to $\frac{1}{2}$, but this does not appear to have any obvious dimensional significance.

It should be noted here that visual range and extinction coefficient become largely dependent on other factors, notably water vapour, when snowfall is very light.

The discrepancy between σ_0 and σ_m is apparently due mainly to a gradient of sky brightness above the hill-tops used as targets. Contrast was measured between the target and the sky a few degrees of elevation above it, while the visual estimates depended on contrast between the target and the sky immediately adjacent to it. Measurements showed that sky brightness immediately above a hill-top was significantly lower than that a few degrees higher, probably because of the low albedo of the broad hill-top. This effect is roughly comparable to the "water sky" phenomenon known to polar navigators. A less important factor was the inherent contrast of the targets C_0; instead of the assumed value -1, C_0 was measured at values close to $-0\cdot9$ for each of the three filters.

Targets of small horizontal extent should not disturb the sky brightness, and therefore the values of σ_0 obtained from the data of Budd and others are probably close to the true values. When corrected coefficients σ_m from this study are compared with the σ_0 values for the Antarctic blizzard, they are of the same magnitude in the range of snow densities common to both studies.

The simple photometric measurements gave no significant correlation between extinction and wave-length in the narrow range observed ($\approx 0\cdot4\ \mu$–$0\cdot6\ \mu$).

MS. received 17 September 1965

REFERENCES

Budd, W., *and others*. In press. The Byrd snow drift project—outline and basic results, by W. Budd, R. Dingle and U. Radok. (*In* Rubin, M., *ed.* Meteorology of the Antarctic. Washington, D.C., American Geophysical Union. (Antarctic Research Series, Vol. 7.))

Johnson, J. C. 1954. *Physical meteorology*. Cambridge, Mass., The M.I.T. Press.

Liljequist, G. H. 1957. Energy exchange of an Antarctic snow-field. Wind structure in the low layer (Mandheim, 71° 03′ S, 10° 56′ W). *Norwegian–British–Swedish Antarctic Expedition, 1949–52. Scientific Results* (Oslo, Norsk Polarinstitutt), Vol. 2, Pt. 1C, p. 185–234.

Mason, B. J. 1962. *Clouds, rain and rainmaking*. Cambridge, University Press.

Middleton, W. E. K. 1952. *Vision through the atmosphere*. Toronto, University of Toronto Press.

APPENDIX

RESULTS OF OBSERVATIONS

A.　VISUAL RANGE DATA.

Date 1964/65	Visual range km.	Accumulation rate g. cm.$^{-2}$ hr.$^{-1}$	Fall velocity cm. sec.$^{-1}$	Snow density g. m.$^{-3}$	Snow type
4/12	1·2	0·104	134	0·216	0·4 mm. crystals clustered into 1 mm. groups and singly
4/12	1·4	0·195	140	0·387	0·4 mm. crystals clustered into 1 mm. groups and singly
6/12	7·2	0·00391	61	0·0178	Hexagonal "flowers" approx. 1 mm. dia.
6/12	3·9	0·00618	61	0·0281	Hexagonal "flowers" approx. 1 mm. dia.
15/12	2·7	0·00924	46	0·0558	Small flakes of stellar crystals $\sim <$ 1 mm. dia.

Date 1964/65	Visual range km.	Accumulation rate g. cm.$^{-2}$ hr.$^{-1}$	Fall velocity cm. sec.$^{-1}$	Snow density g. m.$^{-3}$	Snow type
20/12	7·2	0·00308	70	0·0122	Flakes up to 1 cm. dia. consisting of stellar crystals 1–2 mm. dia.
20/12	1·1	0·0695	81	0·238	Flakes approx. 1 cm. dia. with stellar crystals approx. 2 mm. dia.
20/12	1·5	0·0283	81	0·097	Flakes approx. 1 cm. dia. with stellar crystals approx. 2 mm. dia.
22/12	3·2	0·0252	90	0·0778	0·6 mm. rimed pellets
22/12	3·5	0·0284	80	0·0986	0·7 mm. pellets and 1 mm. "flowers"
22/12	2·9	0·0448	102	0·122	1 mm. "flowers"
22/12	2·4	0·0522	78	0·186	Flakes approx. 1 cm. consisting of stellar crystals approx. 1 mm.
22/12	1·2	0·110	66	0·464	Flakes approx. 1 cm. consisting of stellar crystals approx. 1 mm. (slight wind)
13/1	3·0	0·0423	61	0·193	0·5 mm. prisms and granules with some denritic growth
13/1	2·6	0·0423	49	0·240	0·5 mm. prisms and granules with some denritic growth
16/1	3·5	0·0311	71	0·122	0·3 mm. dia. spatial dendrites
16/1	2·15	0·0490	75	0·181	0·7 mm. dia. spatial dendrites
16/1	3·0	0·0277	91	0·0846	0·2–0·5 mm. spatial dendrites
17/1	7·0	0·0048	61	0·0219	Flakes consisting of plane dendrites 4 mm. dia.
20/1	1·6	0·101	68	0·413	0·8 mm. spatial dendrites
20/1	1·9	0·0589	81	0·202	Flakes approx. 0·5–1·0 cm. consisting of plane dendrites 2 mm.
24/1	1·7	0·087	97	0·249	Fine needles, 2 mm. long and 0·1 mm. thick. Also 0·8 mm. dendrites or perhaps cores of larger shattered stars, clumping into flakes
24/1	1·8	0·052	98	0·147	Clumped spicules, each 2 mm. long, 0·1 mm. thick
26/1	1·4	0·129	91	0·393	Flurrying flakes of 1 mm. spatial dendrites
5/2	4·5	0·0114	52	0·0609	0·2 mm. dia., granular
5/2	3·8	0·0136	49	0·0771	0·1–0·7 mm. dia., granular
10/2	2·0	0·269	122	0·611	2 mm. long needles and ice granules clumping into flakes
18/2	3·4	0·0336	70	0·133	1 cm. flakes consisting of approx. 3 mm. dia. stellar dendrites
18/2	1·8	0·106	70	0·421	1 cm. flakes consisting of approx. 3 mm. dia. stellar dendrites
18/2	0·8	0·158	70	0·627	1–2 mm. dia. stars and flakes ≤ 1 cm. dia.
18/2	0·5	0·196	70	0·778	1–2 mm. dia. stars and flakes ≤ 1 cm. dia.
22/2	1·6	0·104	94	0·307	Flakes ≤ 1 cm. dia. consisting of spatial dendrites approx. 2 mm.
22/2	1·2	0·107	73	0·407	Flakes ≤ 1 cm. dia. consisting of spatial dendrites approx. 2 mm. (slight turbulence)
26/2	1·3	0·118	98	0·333	Refrozen granules and flakes (evidence of prior melting)
26/2	1·1	0·153	106	0·401	Iced crystals approx. 1 mm. dia.
10/3	7·5	0·0056	76	0·0204	Fine granules and dendrites
20/3	7·0	0·00294	61	0·0134	0·5 mm. spicules and approx. 1 mm. aggregations
20/3	4·6	0·00594	72	0·0229	Approx. 2 mm. aggregations of spicules and spatial dendrites
23/3	2·2	0·0251	81	0·086	Flakes > 1 cm. consisting of stellar dendrites 4–5 mm. dia.
23/3	1·9	0·0288	87	0·092	Flakes > 1 cm. of stellar dendrites approx. 5 mm. dia.
23/3	3·6	0·0258	90	0·0796	Flakes approx. 1 cm. of stellar dendrites approx. 4 mm. dia.
23/3	3·8	0·0166	81	0·0570	Flakes approx. 1 cm. and stars 4 mm. dia.

Date 1964/65	Visual range km.	Accumulation rate g. cm.$^{-2}$ hr.$^{-1}$	Fall velocity cm. sec.$^{-1}$	Snow density g. m.$^{-3}$	Snow type
23/3	5·2	0·0125	84	0·0413	Flakes < 1 cm. and stars 4 mm.
23/3	6·5	0·0036	70	0·0143	1 mm. spatial dendrites and 2–3 mm. aggregations
23/3	2·2	0·0177	64	0·0768	Plane "flowers" and spicules ⩽ 1 mm.
23/3	3·4	0·0207	70	0·082	Plane "flowers" and spicules ⩽ 1 mm.
26/3	4·4	0·102	94	0·301	Flakes approx. 1 cm. ("warm")
26/3	4·6	0·0966	101	0·266	Rimed stars ⩽ 5 mm.
26/3	3·4	0·125	87	0·517	Rimed crystals and aggregations < 1 cm. dia.
26/3	2·2	0·150	122	0·341	Flakes ⩾ 1 cm.
29/3	0·8	0·138	81	0·472	Mainly 4 mm. flakes with 1 mm. spatial dendrites
29/3	3·0	0·0485	84	0·160	0·5 mm. spatial dendrites, few small flakes
29/3	2·7	0·0945	87	0·302	1 mm. rimed spatial dendrites
29/3	1·4	0·116	70	0·460	Rimed dendrites, 1–2 mm. dia.
29/3	1·1	0·175	74	0·657	Rimed dendrites, 1–2 mm. dia., also capped columns
29/3	0·75	0·232	94	0·686	1–2 mm. dia. dendrites

B. PARTICLE CONCENTRATION

Date 1965	Vertical flux cm.$^{-2}$ sec.$^{-1}$	Fall velocity cm. sec.$^{-1}$	Concentration dm.$^{-3}$	Density g. m.$^{-3}$	Snow type
16/1	0·546	71	7·7	0·122	0·3 mm. spatial dendrites
16/1	1·40	91	15·4	0·0846	0·2–0·5 mm. spatial dendrites
20/1	0·656	68	9·64	0·413	0·8 mm. spatial dendrites
24/1	0·996	97	10·3	0·249	Fine needles 2 mm. long, 0·1 mm. thick. Also 0·8 mm. dendrites or fragments
24/1	0·586	98	5·97	0·147	Clumped spicules, each 2 mm. long, 0·1 mm. thick
5/2	0·396	52	7·62	0·0609	0·2 mm. dia. grains
5/2	0·495	49	10·1	0·0771	0·1–0·7 mm. grains
20/3	0·156	61	2·56	0·0134	0·5 mm. spicules and 1 mm. aggregations
20/3	0·363	72	5·04	0·0229	2 mm. aggregations of spicules and spatial dendrites
23/3	2 × 10^{-3}	87	0·0230	0·092	Flakes > 1 cm. of stellar dendrites approx. 5 mm.
23/3	2 × 10^{-3}	81	0·0247	0·086	Flakes > 1 cm. of plane dendrites 4–5 mm. dia.
26/3	5 × 10^{-3}	122	0·0410	0·341	Flakes > 1 cm. of stellar dendrites
29/3	0·438	84	5·21	0·160	0·5 mm. spatial dendrites with few small flakes
29/3	0·581	87	6·68	0·302	1 mm. rimed spatial dendrites
29/3	0·476	70	6·80	0·460	Rimed dendrites, 1–2 mm.
29/3	0·371	74	5·01	0·657	Rimed dendrites, 1–2 mm. dia., and capped columns
29/3	1·18	94	12·5	0·686	1–2 mm. dendrites

C. ESTIMATED PARTICLE MASS

Snow type	Approximate mean particle mass g.
0·3 mm. dia. spatial dendrite	1·47 × 10^{-5}
0·2–0·5 mm. dia. spatial dendrite	5·5 × 10^{-6}
0·8 mm. dia. spatial dendrite	4·29 × 10^{-5}
0·2 mm. dia. rimed grains	7·99 × 10^{-6}
0·1–0·7 mm. rimed grains	7·63 × 10^{-6}
0·5 mm. dia. spatial dendrites	3·07 × 10^{-5}
1 mm. rimed spatial dendrites	4·52 × 10^{-5}
1–2 mm. rimed plane dendrites	5·49 × 10^{-5}
1 mm. dia. hexagonal "flowers" (plane dendrites with plates on arms)	2 × 10^{-6}
1 mm. stellar dendrites	1·5 × 10^{-6}
1–2 mm. dia. stellar dendrites	5 × 10^{-6}
Needles, 2 mm. long, 0·1 mm. thick	1·4 × 10^{-5}